Comparisons of Initial condition perturbation methods for regional ensemble wind speed forecasts in Gansu, China

Zifen Han[1,*], Diangang Hu[1], Jianmei Zhang[2], Qingquan Lv[2]

[1]State Grid Gansu Electric Power Company, Lanzhou, China
[2]State Grid Gansu Electric Power Company, Electric Power Research Institute, Lanzhou, China

*wujiexia0102@163.com

Abstract. The study examined three methods for developing a regional ensemble prediction system (EPS) to forecast wind speeds: dynamical downscaling, breeding of growth modes (BGM), and blending. We used the Weather Research and Forecasting (WRF) model to downscale the ensemble forecasts of the European Centre for Medium-Range Weather Forecasts (ECMWF) over Gansu province, China. One-month tests between October 1st and October 31st, 2020, were conducted to assess the performance of the three methods.

The results show that the blending method combines the high-resolution WRF BGM ensemble's small-scale features and the global ensemble's large-scale features, making it superior to the other two methods. Moreover, the performance difference is mainly observed in forecast and becomes less significant as the forecast time increases.

Additionally, we proposed an alternative method for generating scaling factors to eliminate the dependency on observation data, as the BGM method requires such data for generating scaling factors.

Keywords: ensemble, dynamical downscaling, BGM, blending.

1 Introduction

The Global Wind Energy Council reported that the total global capacity of wind power has reached a significant milestone of 837 GW(GWEC2022). Wind energy will very likely maintain its strong growth momentum and play a dominant role in facilitating the world's transition to a low-carbon or net-zero future. However, the penetration of wind power also presents many challenges due to it's fluctuating and intermittent power generation [34]. Accurate wind forecast plays a crucial role in resolving these challenges [9, 12, 23]. Accurate wind forecast is essential in diminishing grid stress and reserve requirements [30].

Wind forecasting has mainly three classes of methods: statistical methods relying on historical data, physics-based numerical weather prediction (NWP) models, and hybrid approaches. The importance of different methods varies with the forecast lead time

A. E. Abomohra et al. (eds.), *Proceedings of the 2023 9th International Conference on Advances in Energy Resources and Environment Engineering (ICAESEE 2023)*, Atlantis Highlights in Engineering 29,
https://doi.org/10.2991/978-94-6463-415-0_21

[32]. A recent systematic review by Hanifi et al. [17] concluded that NWP models significantly benefit forecasts beyond 6 hours. However, NWP simulations suffer from uncertain that result from the initial conditions, limited understanding of the atmosphere's physical process[13,41]. The ensemble prediction system (EPS) is a promising approach to estimate forecast uncertainties [1,14]. The construction of EPS involves perturbing the initial conditions, which is commonly adopted by several global operational ensemble forecasting centers[28,39]. However, the methods used to perturb initial conditions may vary among these centers.

Toth and Kalnay [36] introduced the breeding of growth modes (BGM) method at the National Centers for Environmental Prediction (NCEP), previously known as the National Meteorological Center (NMC)[6]. The European Centre for Medium-range Weather Forecast (ECMWF) developed and implemented the Singular Vector (SV) method, which identifies the fastest-growing directions[7]). Also, the Canadian Meteorological Centre (CMC) developed an ensemble data assimilation method to create diverse initial conditions for ensemble forecasts[20,21]. Because of the limited computing resources, the global EPS is generally operated at coarser resolutions than their deterministic counterparts. For example, the NCEP global ensemble forecast system (GEFS) operates has a horizontal resolution of 34 km [46], while the NCEP Global Forecast System (GFS) runs at a 28 km horizontal resolution. In contrast, the ECMWF EPS has the highest horizontal resolution of the global EPS, with a horizontal resolution of 18 km and 91 vertical levels, including one control member and 50 perturbed members[5,26].

The region of interest for this study, Gansu province in China, has abundant wind resources and houses the world’s largest onshore wind farms. However, Gansu faces the most significant wind curtailment in China, with over 10.4 TW h of potential wind power being wasted in 2016 [11]. Lew et al. [25] found that a 10% improvement in wind forecasts could result in a 4% reduction in curtailment and operation costs. Therefore, improving wind forecasts for Gansu wind farms is essential. In addition, the complex topography of northwest China's Gansu province necessitates higher spatial resolutions to address the impact of topography[31,45].

Because of the coarse horizontal resolution of the global EPS, a regional EPS needs to be constructed to achieve an accurate wind forecast[35]. The accuracy of a regional EPS significantly depends on the proper construction of the initial condition perturbations and lateral boundary condition (LBC) perturbations. Dynamically downscaling a global EPS to the regional domain is the most widely used approach [40]. Due to its simplicity and low computational costs, many NWP centers use this method for regional operational EPS [3,15,44]. Nonetheless, the dynamical downscaling method is unable to capture the small-scale uncertainties that the regional model resolves [27]. Consequently, researchers utilize modified versions of traditional perturbation methods, such as BGM, SV, and ensemble transform Kalman filter (ETKF)[4], that provide more information regarding small-scale uncertainties. Caron et al. [8] reported that spurious perturbations occur due to mismatches between the initial condition perturbations and the LBC perturbations. Therefore, a blending method was proposed that combines small-scale initial condition perturbations based on the regional model and large-scale perturbations from the global EPS [37,38]. Zhang et al. [42] also showed that the

breeding method enhanced the ensemble spread and forecast skills of the Global/Regional Assimilation and Prediction Enhanced System (GRAPES) Regional EPS (GRAPES-REPS).

In this study, we use the Weather Research and Forecasting (WRF) model for the dynamical downscaling of ECMWF EPS to generate large-scale perturbations and the BGM method to generate small-scale initial condition perturbations because of its clarity and low computational cost. Since the BGM method calculates scaling factors using forecast error, and observations are not always accessiable, we proposed an alternative approach for the scaling factor calculation. Besides, the study employs the blending method to merge perturbations of varying dimensions, and the wind forecast performance of dynamical downscaling, BGM, and blending in Gansu is compared.

The paper is structured as follows: Section 2 describes the WRF model setup and regional EPS using dynamical downscaling, BGM, and blending methods. Section 3 introduces data and evaluation metrics. Section 4 outlines the day-ahead and ultra-short wind forecasts conducted over a month. Finally, section 5 concludes the study with recommendations for future research based on the results.

2 WRF model setup and perturbation methods description

2.1 WRF model setup

The WRF model version 3.9.1 is used. The model is configured with a single domain at a horizontal grid resolution of 8 km, as illustrated in Fig.1, centered at 38°N in latitude and 101°E in longitude. The model adopted a terrain-following vertical coordinate with 55 vertical levels and a model top at 50 hPa. The WRF model was run only with the ECMWF EPS initialized at 12 UTC, which is run four times per day, for 54 hours of forecasts. The physics parameterizations are chosen following the method mentioned in [22]. The selected schemes include WRF Single-Moment 6-Class for microphysics[19], Bougeault-Lacarrère (BouLac) planetary boundary layer (PBL) scheme [2], Pleim-Xiu land surface model [29], Kain-Fritsch scheme for cumulus[24], and New Goddard for both longwave and shortwave radiation[10].

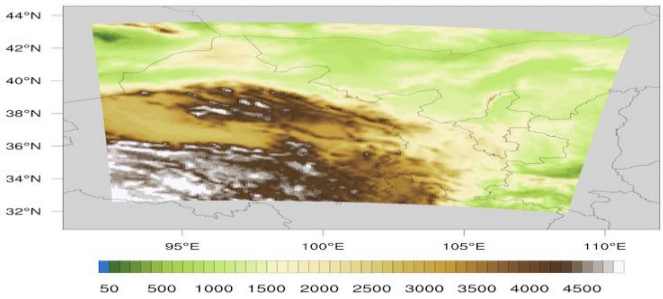

Fig. 1. Digital elevation data of the single WRF domain with horizontal resolution at 8 km.

2.2 Description of the initial condition perturbation methods

This study compared three initial condition perturbation methods: dynamical downscaling, BGM, and blending. The WRF model is used for dynamically downscaling all the 51 ensemble members of ECMWF EPS for initial condition and LBC perturbations. Table 1 provides a summary of these methods.

Table 1. Description of experiments including downscaling, BGM and blending

Experiment	Initial condition perturbation	Lateral condition perturbation
Downscaling	Dynamical downscaling of ECMWF EPS	ECMWF EPS
BGM	WRF BGM	ECMWF EPS
Blending	Blending ECMWF EPS with WRF BGM	ECMWF EPS

BGM method.

The BGM method is a widely used initial condition perturbation technique for ensemble prediction. In this study, the classic BGM method is implemented following Toth and Kalnay. Firstly, an initial random perturbation determined by Eq.1.

$$P(z) = \omega RE(z) \tag{1}$$

where z represents the state variable of the NWP model (z could be thermal and dynamic fields as T U, or V, respectively), and ω is an adjustment coefficient to control the magnitude of the initial random perturbations. R is a uniformly distributed random number in the interval [-1, 1]. E(z) is the root mean square error (RMSE) for variables at each layer.

Next, the model with both the unperturbed and perturbed initial condition is run for a short period (i.e. 12 hours for all the experiments in this paper). Then, the difference between the control prediction with an unpVerturbed initial condition and the perturbation prediction with an unperturbed initial condition is calculated. This scaled difference is added to the analysis of the succeeding time t+1. The process is repeated forward in time to generate the final perturbations until the growth rate of perturbations reaches saturation. The detailed calculations of perturbations are as follows:

$$p_{t+1} = c_t(f_t^a - f_t^s) \tag{2}$$

$$c_t = E(p_t)/E(p'_{t+1}) \tag{3}$$

where $p_{t+1}$is the perturbation at time t+1 of the next cycle; f_t^a and f_t^s represent the perturbed and control predictions, respectively. Meanwhile, c_t is the scaling factor, while p_t and p'_{t+1} are RMSE at the beginning and end of the cycle period, respectively.

Traditionally, the calculation of the scaling factor requires observation data. However, since observation data is not always available, we propose the use of the min-max scaling technique to scale the perturbations between -a and a without observations. This

technique, a normalization technique widely used in machine learning, is easily applicable and requires no knowledge of the statistical properties of the perturbations (Eq.4).

$$p_{t+1} = \frac{p' - \min(p'_{t+1})}{\max(p'_{t+1}) - \min(p'_{t+1})} 2a - a \tag{4}$$

where $a = \omega E(z)$ to ensure that the amplitude of perturbations of the final perturbations at the end of the cycle matches the initial perturbations.

Blending.

The blending method combines small-scale uncertainties resolved by the WRF BGM with large-scale features from ensemble forecast. Also, incorporating perturbations from the global ensemble in the initial condition perturbation ensures consistency between the initial condition and the LBC provided by the global ensemble.

This blending method follows these steps: firstly, using the WRF model to downscale the global ensemble initial condition to the regional domain to obtain large-scale uncertainties; secondly, adding these downscaled initial conditions to the perturbations generated by the WRF BGM as described in Section 2.2.

3 Data and metrics for evaluation

3.1 Observation data

From October 1st, 2020, to October 31st, 2020, the study evaluates the hourly wind speed observations at wind turbine hub height from 28 wind farms in Gansu, China, using the WRF model's output. The WRF model output is interpolated to the turbine hub height to compare with observation data. In addition, the wind speed forecast of the nearest grid point in the WRF domain is extracted to compare with wind turbine observations.

3.2 Evaluation methods

The National Energy Bureau (NEB) requires day-ahead short-term and four-hours ahead wind forecasts are required (Chinese GBT). We use the 12 UTC ECMWF data to generate these forecasts, with forecast horizons ranging from 28 to 51 hours for day-ahead forecasts and 10 to 13 hours for ultra-short term forecasts.

To evaluate the performance of ensemble forecasts generated by the three initial condition perturbation methods, we applied several verification methods, such as RMSE and mean bias error (MBE) for the ensemble mean, standard deviation (std) for ensemble spread, continuous ranked probability score (CRPS) [18,33], and rank histograms[16]. These measures are calculated using the 1-hourly wind speed forecasts following the equations mentioned below:

$$RMSE = \sqrt{\sum (WS_{pred} - WS_{obs})^2 / N} \tag{5}$$

$$MBE = \frac{1}{N}\sum(WS_{pred} - WS_{obs}) \tag{6}$$

$$std = \sqrt{\sum(x_{pred} - \overline{x_{pred}})^2} \tag{7}$$

where WS_{pred} and WS_{obs} are the predicted and observed wind speed *WS*, respectively. *N* is the number of forecast and observation pairs. x_{pred} represent forecasted values by a single ensemble member, and $\overline{x_{pred}}$ represent mean forecast of the ensemble. RMSE and MBE of the ensemble mean measure the deterministic skill of the ensemble forecast. Additionally, the std of the ensemble members in relation to the ensemble mean is defined as the ensemble spread. In the absence of observations, the ensemble spread can be used as a predictor of skills of the ensemble mean, as proposed by Whitaker et al.[41]. Lower values of spread suggest low uncertainties, while higher values suggest the opposite.

The CRPS is defined as:

$$CRPS = \sum_{-\infty}^{\infty}[F(y) - F_o(y)]^2 dy \tag{8}$$

where $F_o(y)$ is an indicator function of which the value is 0 if the forecast variable y is less than the observation and 1 otherwise (Eq.9).

$$F_o(y) = \begin{cases} 0, & if\ y < observed\ value \\ 1, & otherwise \end{cases} \tag{9}$$

The smaller the value of the CRPS, the better the ensemble forecast, as the CRPS measures forecast accuracy. To calculate the CRPS in this study, the properscoring package in Python is used.

The rank histogram is another valuable tool for evaluating ensemble reliability by sorting each ensemble member's forecast values relative to the rank of the verification, often the observation, in ascending order[45]. A flat rank histogram indicates a perfect EPS. However, a U-shaped rank histogram generally suggests deficient variability in the ensemble forecast, and an asymmetric shape (whether J or L-shaped) implies bias.

4 Results and discussion

Fig. 2 illustrates a comparison of the one-month averaged CRPS and ensemble spread of wind speed forecasts as a function of forecast horizon, ranging from 10 to 54 hours of downscaling (solid purple), breeding (dashed green), and blending (dashed red) of the ECMWF-EPS. Overall, the blending methods performs best, generating the smallest CRPS values and largest ensemble spread, particularly for the forecast lead time between 10 and 25 hours. The BGM ensemble follows closely with slight improvements in early forecast lead time, as evidenced by a lower RMSE and larger spread. Since all three ensembles use the same LBCS from ECMWF-EPS forecasts, it is evident that the BGM method is superior to the downscaling method while the blending method benefits from both perturbation methods. The distinction in CRPS and ensemble spread among downscaling, BGM, and blending become negligible after 25 hours. The results suggest that the long-term forecasts within the study domain are mostly influenced by

physics and boundary conditions dominate over initial condition perturbations. Fig. 3 shows that the the ensemble mean's RMSE and MBE are almost identical in downscaling, BGM, and blending ensembles. However, the blending ensemble exhibits slightly lower values than the downscaling and BGM ensembles during the early forecast lead time.

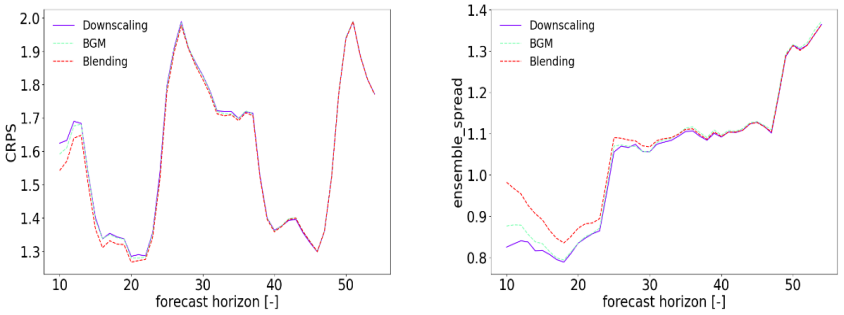

Fig. 2. One-month averaged CRPS and ensemble spread as a function of forecast lead time from 10 to 54 hours wind speed forecast for the downscaling, BGM, and blending ensembles over 28 wind farms in Gansu, China.

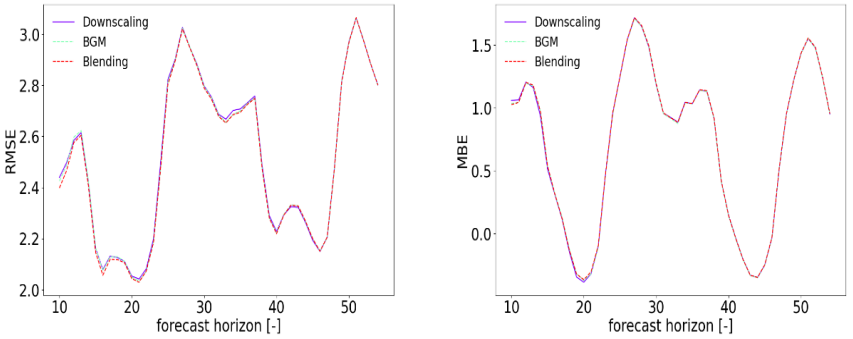

Fig. 3. One-month averaged RMSE and MBE as a function of forecast lead time from 10 to 54 hours wind speed forecast for the downscaling, BGM, and blending ensembles over 28 wind farms in Gansu, China.

Fig. 4 compares the rank histogram for the wind speed forecasts with forecast lead time ranging from 10 to 54 hours among the downscaling (blue), BGM (green), and blending (red) ensembles. All three ensembles exhibit a U-shaped rank histogram, indicating that the ensemble forecasts are under dispersive. However, the blending ensemble achieves a flatter rank histogram than the downscaling and BGM ensembles, indicating the highest frequency of observations lying inside it. Compared to downscaling, the BGM ensemble is also relatively flatter.

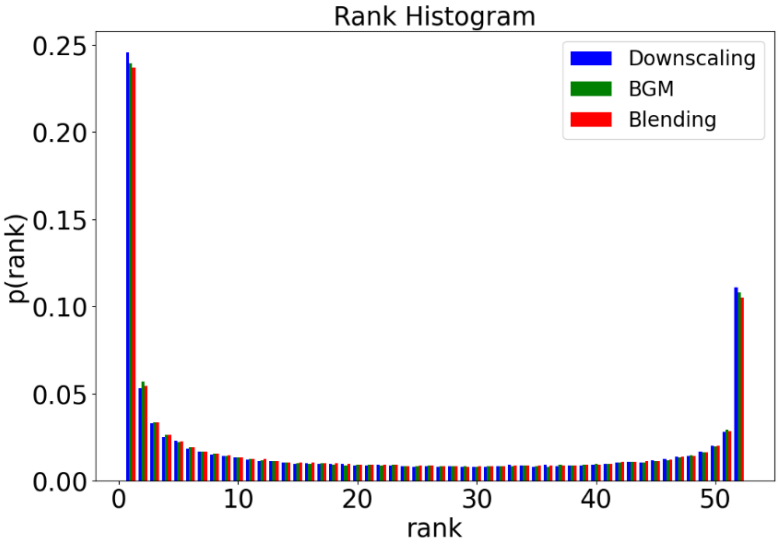

Fig. 4. Rank histogram for wind forecast of forecast lead time from 10 to 54 hours for the downscaling, BGM, and blending ensembles over 28 wind farms in Gansu, China.

Table 2 summarizes the one-month averaged RMSE and MBE of the ensemble mean for wind speed forecasts of the downscaling, BGM, and blending ensembles over forecast horizons ranging from 10 to 13 hours and 28 to 51 hours. The blending ensemble boasts a smaller RMSE, particularly over the earlier forecast lead time of 10 to 13 hours, compared to the other two ensembles, consistent with Fig. 3.

Table 2. RMSE and MBE of the ensemble mean for wind speed forecasts of the downscaling, BGM, and blending ensembles averaged over forecast lead time of 10 to 13 hours and 28 to 51 hours.

	10 to 13 hours			28 to 51 hours		
	Downscaling	BGM	Blending	Downscaling	BGM	Blend-ing
RMSE	2.531	2.530	2.508	2.582	2.579	2.577
MBE	1.122	1.112	1.113	0.722	0.721	0.725

The analysis presented above reveals the superiority of the blending ensemble over the downscaling and BGM ensemble. Additionally, the improvement in the effect of BGM and blending is notable in the earlier forecast lead time of 25 hours or less. However, if the domain of the study expands, the impact may extend to a more extended lead time, as LBCs will take more time to dominate over initial condition perturbations (this is beyond the scope of this study, thus not shown). Therefore, applying the blending method is worthwhile, despite the minimal improvement in RMSE, to improve regional EPS reliability[43].

5 Conclusions

This study examines three methods of generating initial condition perturbations for the Gansu Province of China's ensemble wind speed forecasts: dynamical downscaling, BGM, and blending. Dynamical downscaling generates large-scale perturbations by directly downscaling the ECMWF EPS using the WRF model. Since the required observation data is not available for the BGM method to generate the periodic scaling factor, we suggest using the min-max scaling method to scale small-scale perturbations. The WRF BGM method can resolve small-scale perturbations, whereas the blending method can combine both large and small perturbations. During the one-month testing period of October 1st to October 31st, 2020, the blending ensemble demonstrated the best forecast skill, particularly at the early forecast lead time. The probabilistic forecast of the blending ensemble is better demonstrated by the CRPS, ensemble spread, and rank histogram of wind speed forecasts. Furthermore, the difference among the three perturbation methods decreases as the forecast lead time becomes insignificant after 25 hours. The RMSE and MBE comparisons of wind speed forecast also support the conclusion that the blending ensemble is superior to downscaling and BGM ensembles.

Acknowledgements

The authors acknowledge Envision Group Pte. Ltd. and State Grid Gansu Electric Power for the support and funding.

Funding

State Grid Gansu Electric Power Company science project “The application of renewable energy on electric power generation”(522722220025).

Reference

1. Parker D J, Blyth A M, Woolnough S J, et al. The African SWIFT project: growing science capability to bring about a revolution in weather prediction[J].Bulletin of the American Meteorological Society. DOI:10.1175/BAMS-D-20-0047.1 (2021).
2. Singh P, Ahrens B.: Modeling Lightning Activity in the Third Pole Region: Performance of a km-Scale ICON-CLM Simulation (2023).
3. Bowler, E., Arribas, A., Mylne, K., Robertson, K., Beare, S.: The mogreps short-range ensemble prediction system. Quarterly Journal of the Royal Meteorological Society: A journal of the atmospheric sciences, applied meteorology and physical oceanography, 134(632), 703–722 (2018).
4. Mamgain A, Sarkar A, Rajagopal E N.: Medium-range global ensemble prediction system at 12km horizontal resolution and its preliminary validation[J]. Meteorological Applications, 27(1).DOI:10.1002/met.1867 (2020).

5. Buizza, M. F., R., Palmer, T. N., Petroliagis, T.: The ecmwf ensemble prediction system: Methodology and validation. Quarterly Journal of the Royal Meteorological Society, 122(529),73–119 (1996).
6. Wang L, Robertson A W, Week 3–4 predictability over the United States assessed from two operational ensemble prediction systems. Climate Dynamics, DOI:10.1007/s00382-018-4484-9 (2019).
7. Buizza. R and Palmer, T.: The singular-vector structure of the atmospheric global circulation. Journal of Atmospheric Sciences, 52(9), 1434 – 1456 (1995).
8. Keresturi, EndiWang, YongMeier, FlorianWeidle, FlorianWittmann, ChristophAtencia, Aitor.Improving initial condition perturbations in a convection-permitting ensemble prediction system. Quarterly Journal of the Royal Meteorological Society, 145 (2019).
9. Chang, G.W., Lu, H.J., Chang, Y.R., Lee., Y.D.: An improved neural network-based approach for short-term wind speed and power forecast. Renewable Energy, 105,301–311 (2017).
10. Chou, M., Suarez, M. A solar radiation parameterization for atmospheric studies. Technical report (1999).
11. Dong, C., Qi, A., Dong, W., Lu, X., Liu, T., Qian, S.: Decomposing driving factors for wind curtailment under economic new normal in china. Applied Energy, 217,178–188 (2018).
12. Zhang Y M, Wang H, Lund H, et al. Multi-head attention-based probabilistic CNN-BiLSTM for day-ahead wind speed forecasting (2023).
13. Edward N., Deterministic nonperiodic flow. Journal of Atmospheric Sciences, 20(2), 130 – 141(1963).
14. Gneiting, T., and Raftery, A.: Weather forecasting with ensemble methods. Science, (5746), 248–249 (2005).
15. Hagelin, S., Son, J., Swinbank, R., McCabe, A., Roberts, N., Tennant, W.: The met office convective-scale ensemble, mogreps-uk. Quarterly Journal of the Royal Meteorological Society, 143(708), 2846–2861 (2017).
16. Hamill, T.: Interpretation of rank histograms for verifying ensemble forecasts. Monthly Weather Review, 129(3), 550–560 (2001).
17. Hanifi, S., Liu, X., Lin, Z., Lotfian, S.: A critical review of wind power forecasting methods - past, present and future. Energies, 13(15), (2020).
18. Hersbach, H.: Decomposition of the continuous ranked probability score for ensemble prediction systems. Weather and Forecasting, 15 (5), 559–570 (2000).
19. Hong, S., and Lim, J.: The wrf single-moment 6-class microphysics scheme (wsm6). Asia-Pacific Journal of Atmospheric Sciences, 42(2), 129–151 (2006).
20. Houtekamer, P., Derome, J.: Methods for ensemble prediction. Monthly Weather Review, 123, 2181–2196 (1995).
21. Houtekamer, P., Lefaivre, L., Derome, J., Ritchie, H., Mitchell, H.: A system simulation approach to ensemble prediction. Monthly Weather Review, 124(6):1225 – 1242 (1996).
22. Matsumoto, T., and Yamada, Y. Comprehensive and Comparative Analysis of GAM-Based PV Power Forecasting Models Using Multidimensional Tensor Product Splines against Machine Learning Techniques. Energies 14 (2021).
23. Latypov S, Savostin A, Kalantayevskaya N. Design of decision-making support system in power grid dispatch control based on the forecasting of energy consumption[J]. Cogent Engineering, 2022, 9(1), DOI:10.1080/23311916.2022.2026554 (2022).
24. Kain, J.: The kain-fritsch convective parameterization: an update. Journal of applied meteorology, 43(1) 170–181 (2004).

25. Kun L I, Chen C, Hongrang H E, et al.Application of Gaussian Weight to Improve Perturbation Features of Convection-Permitting Ensemble Forecast Based on Local Breeding of Growing Modes[J]. Journal of Meteorological Research, 35(3):15 (2021).
26. Mogensen, F. Pappenberger, P, Rabier,F., Richardson, D., Vitart, F., Malardel. S.: Ecmwf activities for improved hurricane forecasts. Bulletin of the American Meteorological Society, 100(3), 445 – 458 (2019).
27. Ono, K., Kunii, M., Honda, Y.: The regional model-based mesoscale ensemble prediction system, meps, at the Japan meteorological agency. Quarterly Journal of the Royal Meteorological Society, 147(734), 465–484 (2021).
28. Xie Y, Li C, Tang G.: A novel deep interval prediction model with adaptive interval construction strategy and automatic hyperparameter tuning for wind speed forecasting[J]. Energy, 216:119179.DOI:10.1016/j.energy.2020.119179 (2020).
29. Pleim, J. and Xiu, J.: Development and testing of a surface flux and planetary boundary layer model for application in mesoscale models. Journal of Applied Meteorology (1988-2005), pages 16–32 (1995).
30. Potter, C., Eric P. Grimit, E. P., and Nijssen, B.: Potential benefits of a dedicated probabilistic rapid ramp event forecast tool. 2009 IEEE/PES Power Systems Conference and Exposition, pages 1–5 (2009).
31. Prósper, M., Carlos, O., Fernández, F., and Gonzalo, M.: Wind power forecasting for a real onshore wind farm on complex terrain using wrf high resolution simulations. Renewable energy, 135, 674–686 (2019).
32. Santhosh, M., Venkaiah, C., Kumar, D.: Current advances and approaches in wind speed and wind power forecasting for improved renewable energy integration: A review. Engineering Reports, 2(6) (2020).
33. Doubleday, K., Jascourt, S., Kleiber, W., & Hodge, B. M.: Probabilistic solar power forecasting using bayesian model averaging. IEEE Transactions on Sustainable Energy, PP(99), 1-1 (2020).
34. Soman, S., Zareipour, H., Malik, O., Mandal, P.: A review of wind power and wind speed forecasting methods with different time horizons. In North American Power Symposium 2010, pages 1–8 (2010).
35. Wastl C, Wang Y, Atencia A, et al.C-LAEF: Convection-permitting Limited-Area Ensemble Forecasting system[J]. Quarterly Journal of the Royal Meteorological Society, 2021.DOI:10.1002/qj.3986 (2021).
36. Toth, Z., and Kalnay, E.: Ensemble forecasting at nmc: The generation of perturbations. Bulletin of the American MeteorologicalSociety, 74(12),2317 – 2330 (1993).
37. Wang Y, Zhang X, Toth Z.: Application of the Bayesian Processor of Ensemble to the Combination and Calibration of Ensemble Forecasts, International conference on signal and information processing, networking and computers(2019).
38. Wastl C, Wang Y, Atencia A.: Independent perturbations for physics parametrization tendencies in a convection-permitting ensemble (pSPPT)[J]. Geoscientific Model Development, 12(1), 261-273.DOI:10.5194/gmd-12-261(2019).
39. Wang, J., Chen, J., Zhang, H., Tian, H., & Shi, Y.: Initial Perturbations Based on Ensemble Transform Kalman Filter with Rescaling Method for Ensemble Forecasting."Weather and Forecasting 3(2021).
40. Weidle, F., Wang, Y., Smet, G.: On the impact of the choice of global ensemble in forcing a regional ensemble system. Weather and Forecasting, 31(2), 515–530 (2016).
41. Whitaker, J., and Loughe, A.: The relationship between ensemble spread and ensemble mean skill. Monthly weather review, 126(12),3292–3302 (1998).

42. Zhang, X.: Impacts of different perturbation methods on multiscale interactions between multisource perturbations for convection-permitting ensemble forecasting during scmrex. Quarterly Journal of the Royal Meteorological Society (2021).
43. Zhang, H., Chen, M., Fan, S.: Study on the construction of initial condition perturbations for the regional ensemble prediction system of north china. Atmosphere, 10(2):87 (2019a).
44. Zhang, H., Pu, Z.: Beating the uncertainties: Ensemble forecasting and ensemble-based data assimilation in modern numerical weather prediction. Advances in Meteorology, 1–10 (2010).
45. Zhang, T., Yan, P., Li, Z., Wang, Y., Li, Y.: Bias-correction method for wind-speed forecasting. Meteorologische Zeitschrift, 28(4), 293–11 (2019b).
46. Wang J W A, Sardeshmukh P D, Compo G P, et al. Sensitivities of the NCEP Global Forecast System[J]. Monthly Weather Review, 147(4).DOI:10.1175/MWR-D-18-0239.1 (2019).